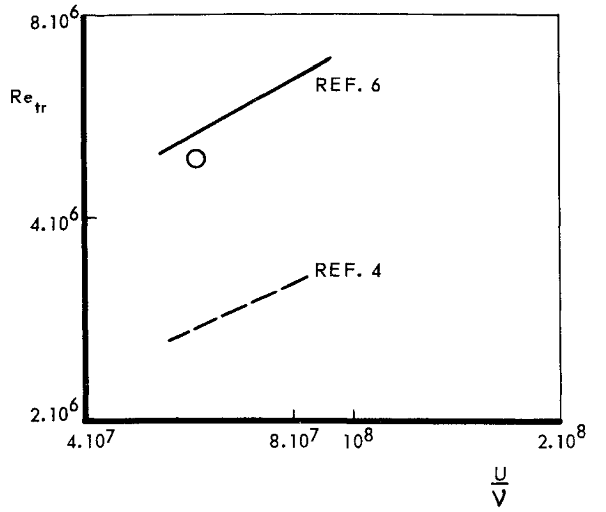

Fig. 3 Transition Reynolds number in 1.20 × 1.20 m² SST compared with correlations.

The prediction is good for the SST (Fig. 3), but about 70% too high for the CSST (Fig. 2).

Conclusions

The present experimental data underline the conclusions from the work of Pate and Schueler[6]: boundary-layer transition in wind tunnels at supersonic speed is not determined by Mach number, unit Reynolds number, and leading edge thickness only, but also by the tunnel environment.

The prediction methods which take the acoustic disturbances from the tunnel wall boundary layer into account (e.g., Ref. 6) predict a difference in the results from both tunnels, but a much smaller one than measured. It is not clear whether this is due to a wrong modelling of the acoustic disturbances or whether any other effect is present.

No decrease in the unit Reynolds number effect was found at very high unit Reynolds numbers, as might be expected on the basis of qualitative arguments.

References

[1] Smith, A. M. O., "Transition Pressure Gradient and Stability Theory," *Proceedings of the 9th International Congress of Applied Mechanics*, Vol. 4, 1957, pp. 234–244.

[2] Van Ingen, J. L., "Theoretical and Experimental Investigations of Incompressible Laminar Boundary Layers with and without Suction," thesis, 1965, Delft University of Technology, Delft, The Netherlands.

[3] Mack, L. M., "The Stability of the Compressible Laminar Boundary Layer according to a Direct Numerical Solution," *Recent Developments in Boundary-Layer Research*, AGARDograph 97—Part I, 1965, pp. 329–362.

[4] Hopkins, E. J., Jillie, D. W., and Sorensen, V. L., "Charts for Estimating Boundary-Layer Transition on Flat Plates," TN D-5846, 1970, NASA.

[5] Nagel, A. L., "Analysis of the Unit Reynolds Number Effect in Hypersonic Flat Plate Boundary-Layer Transition," *Proceedings of the 1968 Heat Transfer and Fluid Mechanics Institute*, edited by A. F. Emery and C. A. Depew, Stanford University Press, Stanford, Calif. 1968, pp. 51–64.

[6] Pate, S. R. and Schueler, C. J., "An Investigation of Radiated Aerodynamic Noise Effects on Boundary-Layer Transition in Supersonic and Hypersonic Wind Tunnels," *AIAA Journal*, Vol. 7, No. 3, March 1969, pp. 450–457.

[7] Ross, R., "A Simple Formula for Flat Plate Boundary-Layer Transition in Supersonic Wind Tunnels," *AIAA Journal*, Vol. 10, No. 3, March 1972, pp. 336–337.

[8] La Graff, J. E., "Experimental Studies of Hypersonic Boundary Layer Transition," thesis, Rept. 1104/70, 1970, Oxford University, Oxford, England.

Density Survey in the Hypersonic Viscous Shock Layer on a Sharp Flat Plate

J. M. Avidor* and S. Lederman†
Polytechnic Insitute of New York, Brooklyn, N.Y.

The hypersonic viscous sharp leading edge flow is a problem of fundamental importance in gasdynamics. The interest in this problem stems from the need to establish the low-density range of validity for the Navier-Stokes equations. Solutions based on the Navier-Stokes formulation are available for the transitional regime[1,2] and a number of investigators have reported surface and flowfield measurements[3,4] which show good agreement with these numerical solutions. Recently, Lewis[5] reported detailed surface and flowfield measurements in the kinetic flow region. Using the relative mean free path, λ_f, originally suggested by Kogan[6] as the scaling parameter for surface transport within the kinetic region, the different flow regimes in the disturbed flow region about the plate were defined. Lewis concluded in this study that the kinetic region extends to about $10\lambda_f$ downstream from the leading edge, followed by the merged region which covers the next $10\lambda_f$. Eventually, at $X \approx 20\lambda_f$, near continuum conditions prevail, and the strong interaction limit is approached. This Note presents experimental results of a density survey in the kinetic through strong interaction regions of a hypersonic sharp flat plate under cold wall ($T_w/T_o = 0.07$) conditions, as well as the correlation of the present and existing data using λ_f rather than the rarefaction parameter, $\bar{V}_{\infty_x} = M(c^*)^{1/2}/(Re_{\infty_x})^{1/2}$, as the scaling parameter. The results show that λ_f correlates the shock strength data remarkably well for over $30\lambda_f$ downstream from the leading edge of the plate.

This investigation was carried out using the electron beam fluorescence technique. This technique originally developed by Muntz[7] has since been used by a number of investigators in the study of rarefied gas flows. The experiments were performed in the PINY 8-ft hypersonic shock tunnel, and a detailed description of the tunnel and electron beam density probe are given in an earlier paper.[8] The measurements were made in nitrogen with a nominal Mach number of 18, with an equilibrium reservoir temperature of about 4000°K, and at one ambient density. This provides a freestream mean free path of 0.012 in. ($Re_\infty = 1500$/in.). Flow conditions were determined from measured values of the incident shock speed, reservoir pressure in the driven tube, and the measured value of the pitot pressure in the test section.

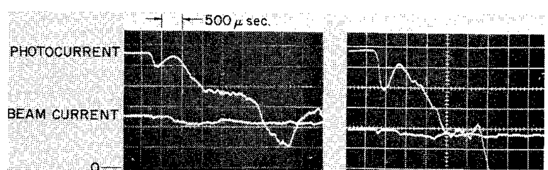

Fig. 1 Photocurrent and beam current during a test.

Presented as Paper 73-690 at the AIAA 6th Fluid and Plasma Dynamics Conference, Palm Springs, Calif., July 16–18, 1973; submitted July 16, 1973; revision received January 8, 1974. This research was conducted in part under Contract Nonr 839 (38) for PROJECT STRATEGIC TECHNOLOGY, supported by the Advanced Research Projects Agency under Order 529 through the Office of Naval Research; and in part under Contract DAHCO4-69-C-0077, monitored by the U.S. Army Research Office—Durham and supported under ARPA Order 1442.

Index categories: Rarefield Flows; Supersonic and Hypersonic Flow; Research Facilities and Instrumentation.

* Formerly Research Associate; presently Senior Scientist, Avco Everett Research Laboratory. Associate Fellow AIAA.

† Professor of Aerospace Engineering. Member AIAA.

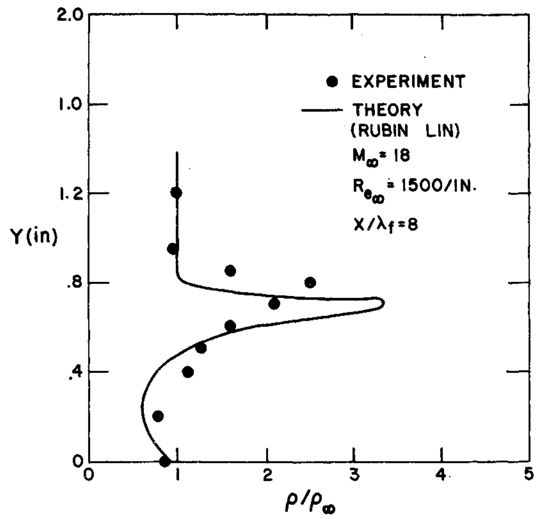

Fig. 2 Density profile at $X = 3$ in.

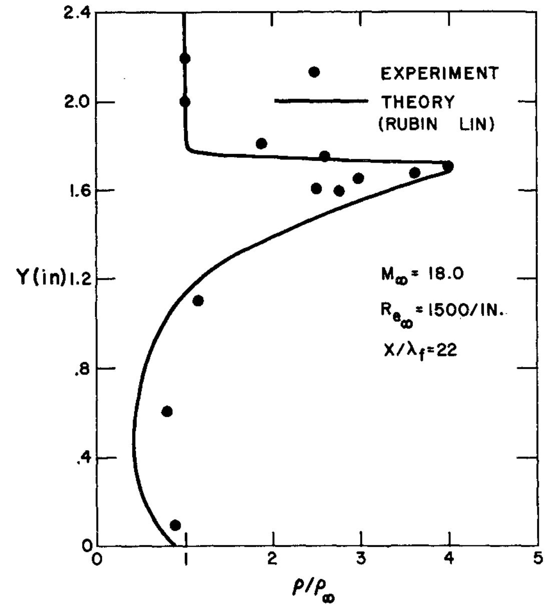

Fig. 4 Density profile at $X = 9$ in.

The flat plate model used in the density survey consisted of a highly polished aluminum sheet $\frac{1}{16}$ in. thick, with a 15° bevel on the undersides, and was 12 in. by 18 in. The plate was connected to the drift tube of the electron gun system and a 2-mm-diam orifice machined into the plate allowed the beam to emerge through the plate and impinge on the beam collector. Since the electron beam density probe was in a fixed position in the tunnel, measurements were made starting with the rear stations and moving forward. As each station was completed, a new orifice was machined at the next location forward. This procedure prevented any disturbances to the measured region from orifices ahead of the testing location.

A series of density profiles normal to the model surface at stations ranging from 2 in. to 9 in. from the leading edge have been obtained. Because of the short test duration, pointwise measurements were made by positioning the electro-optical detector at a different point along the beam in each test. Figure 1 presents typical data traces recorded during a test, the upper trace corresponds to the photomultiplier output, as can be seen after some initial disturbance, there is a gradual increase in the photoluminescence current which, after a certain period of time, levels off to a constant value. The lower trace, which corresponds to the beam current signal, remains relatively constant throughout the test.

Figures 2–4 present the normalized density profiles in the disturbed region about the plate. The density at each point was normalized with respect to the freestream density after corrections were made for changes in beam current between tests and taking into account variation in the photomultiplier output, depending on its position with respect to the plate. Included in these figures are numerical results of the viscous layer solution by Rubin and Lin[1] where rotational nonequilibrium effects on the shock structure have been included. It is evident that relatively good agreement between the experimental and predicted density profiles exist in the viscous layer, slight deviations can be observed in the position of maximum density. However, the absolute values of the theoretical and experimental maximum density value (ρ_{max}/ρ_∞) deviate more significantly, and from Fig. 3, it appears that for $X \geqq 15\lambda_f$, over-all good agreement exists between the measured and calculated density profiles, a result previously observed with Lewis and Harbour data.[4]

Using X/λ_f as the parameter to correlate shock strength data, as shown in Fig. 5, it seems from the present and existing data[4,5,9] that the parameter λ_f correlates the shock strength remarkably well for over $30\lambda_f$ from the leading edge, which covers the near free molecular regime through the merged into the strong interaction region; poor agreement exists with the theoretical result in the region $X < 15\lambda_f$.

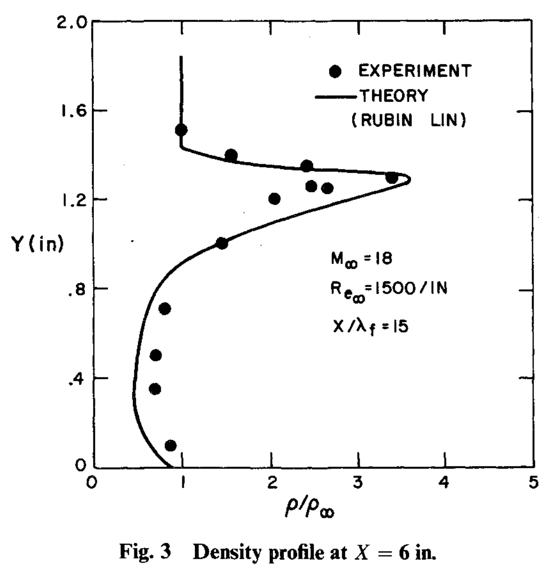

Fig. 3 Density profile at $X = 6$ in.

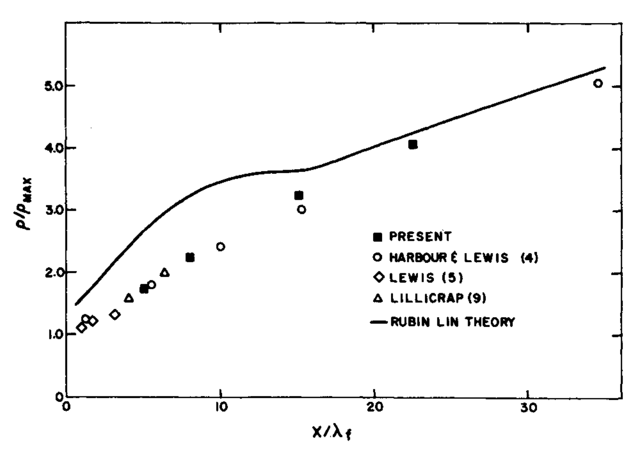

Fig. 5 Correlation of shock strength ρ_{max}/ρ_∞.

In conclusion, it was found in this experimental study of the density distribution in the hypersonic viscous layer that the scaling parameter λ_f correlates the shock strength data remarkably well from the kinetic into the strong interaction region, and that the numerical results based on the Rubin-Lin theory agree well with the experimental data for $X \geqq 15\lambda_f$.

References

[1] Rubin, S. G. and Lin, T., "Rotational Non-Equilibrium Near a Hypersonic Leading Edge," presented at the Seventh International Rarefied Gas Dynamics Symposium, Pisa, Italy, 1970.

[2] Cheng, H. K., Chen, S. Y., Mobly, R., and Huber, C., "On the Hypersonic Leading Edge Problem in the Merged-Layer Regime," *Rarefied Gas Dynamics*, Academic Press, New York, 1969, Suppl. 5.

[3] Vidal, R. J. and Bartz, J. A., "Surface Measurements on Sharp Flat Plates and Wedges in Low-Density Hypersonic Flow," *AIAA Journal*, Vol. 7, No. 6, June 1969, pp. 1099–1109.

[4] Harbour, P. J. and Lewis, J. H., "Preliminary Measurements of the Hypersonic Rarefied Flow Field on a Sharp Flat Plate Using an Electron Beam Probe," *Rarefied Gas Dynamics*, Vol. II, Academic Press, New York, 1967, Suppl. 4.

[5] Lewis, J. H., "An Experimentally Determined Model for the Noncontinuum Flow at the Leading Edge in a High Speed Ratio Stream," Rept. 954, Feb. 1971, Dept. of Aerospace and Mechanical Sciences, Princeton University, Princeton, N.J.

[6] Kogan, M. N., "Hypersonic Nearly Free—Molecule Flows," *Rarefied Gas Dynamics*, Plenum Press, New York, 1969, pp. 443–475.

[7] Muntz, E. P., "Measurement of Rotational Temperature, Vibrational Temperature, and Molecule Concentration in Non-Radiating Flows of Low Density Nitrogen," Rept. 71, April 1961, Univ. of Toronto Institute of Aerophysics, Toronto, Ontario, Canada.

[8] Avidor, J. M. and Lederman, S., "Flowfield Diagnostics in a Rarefied Slightly Ionized Hypersonic Flow," *Israel Journal of Technology*, Vol. 10, No. 1–2, March 1972, pp. 113–121.

[9] Lillicrap, D. C. and Berry, C. J., "Experimental Model for High Speed Rarefied Flow Over a Sharp Flat Plate," *The Physics of Fluids*, Vol. 13, No. 5, May 1970, pp. 1146–1152.

Effect of Axisymmetric Imperfections on the Vibrations of Cylindrical Shells under Axial Compression

AVIV ROSEN* AND JOSEF SINGER†

Technion—Israel Institute of Technology, Haifa, Israel

Nomenclature

C = coefficient in Eq. (5)
c = $[3(1-\nu^2)]^{1/2}$
E = Young's modulus
F = stress function
f = frequency
h = shell thickness
l = shell length
m = mass per unit area
N_x = axial membrane stress resultant
N_y = circumferential membrane stress resultant
N_{xy} = shear membrane stress resultant
n = circumferential wave number
p = axial wave number
R = radius of middle surface of perfect cylindrical shell
T = $(4\rho^4+1)/(4\rho^4+1-4\lambda\rho^2)$
t = time
W = radial displacement (positive outward)
W_o = axisymmetric initial imperfection
w = vibration mode (or buckling mode when frequency is zero)
x = axial coordinate
y = circumferential coordinate
μ = parameter which determines amplitude of imperfection
ν = Poisson's ratio
λ = load parameter, $[3(1-\nu^2)]^{1/2}\sigma R/Eh$
σ = axial compressive stress
ρ^2 = $\{1/[3(1-\nu^2)]^{1/2}\}(h/R)p^2$
ϕ = stress function of additional stress due to vibration (or buckling when frequency is zero)
ω = circular frequency = $2\pi f$
Ω = frequency parameter = $(2\bar{R}^2 m\omega^2/Eh)^{1/2}$
Ω_{min} = lowest frequency parameter for different values of τ at certain load
$(\ )_{,d}$ = differentiation with respect to d
$(\dot{\ })$ = differentiation with respect to time
Δ = Laplacian
τ^2 = $\{1/[3(1-\nu^2)]^{1/2}\}(h/R)n^2$

Received August 20, 1973. The work was supported in part by the Air Force Office of Scientific Research, OAR under Grant AFOSR 72-2394.

Index category: Structural Dynamic Analysis.

* Instructor, Department of Aeronautical Engineering.

† Professor, Department of Aeronautical Engineering.

1. Introduction

SINCE the pioneering work of Koiter in 1945,[1] many studies have emphasized the important role that geometrical imperfections play in the buckling of shells. In particular, cylindrical shells under axial compression have been investigated extensively and the initial geometrical imperfections have been identified there as cause of the large discrepancies between the experimental buckling loads and the theoretical predictions. The present state-of-the-art is that, in most cases, low experimental buckling loads can qualitatively be attributed to initial geometrical imperfections. However, for better quantitative assessments, the nature of the initial imperfections has to be precisely known. From an engineering point of view, it is hence very important to know the precise imperfections of a certain shell or, preferably, the influence of these imperfections without actually buckling the shell, in order to predict the buckling load more accurately. The direct approach of measurement of the deviation of the shape of the structure from its ideal shape has been used in some studies.[2-4] This method is, however, complicated and requires sophisticated equipment and relatively long measurement times. In the present paper, an indirect approach is employed. It is shown that geometrical imperfections of the kind which affect buckling have also a large influence on the vibrations of these shells, even at zero load. This phenomenon facilitates measurement of the actual imperfections by measurement of the deviations in the frequencies of the imperfect shell from those of the corresponding perfect one.

2. Theory

The theoretical development is based on an analysis derived by Koiter.[5] As a matter of fact, the present study essentially only adds the inertia terms to Koiter's formulation. A detailed derivation of the equations is given in Ref. 11, here only the salient features are outlined.

As in Koiter's paper, only axisymmetric imperfections are considered. The equations of the nonlinear theory of shallow shells are employed, and they become in the present case

$$N_x = F_{,yy}, \quad N_y = F_{,xx}, \quad N_{xy} = -F_{,xy} \tag{1}$$

$$(1/Eh)\Delta\Delta F - (1/R)W_{,xx} + W_{o,xx}W_{,yy} + W_{,xx}W_{,yy} - (W_{,xy})^2 = 0 \tag{2}$$

$$[Eh^3/12(1-\nu^2)]\Delta\Delta W + (1/R)F_{,xx} - W_{o,xx}F_{,yy} - W_{,xx}F_{,yy} - W_{,yy}F_{,xx} + 2W_{,xy}F_{,xy} + m\ddot{w} = 0 \tag{3}$$

These equations appear in Koiter's paper[5] without the inertia term of Eq. (3) and are attributed there to Vol'mir.[6] Similar equations were used earlier[7] in the analysis of the nonlinear vibrations of cylindrical shells without consideration of imperfections. Only radial inertia is included here, whereas inplane inertia is neglected. However it was already shown earlier,[8] that for isotropic cylindrical shells consideration of radial inertia only, yields very good results if compared with more exact analysis.